

Available online at www.sciencedirect.com

Procedia Engineering 14 (2011) 1845–1854

**Procedia
Engineering**

www.elsevier.com/locate/procedia

The Twelfth East Asia-Pacific Conference on Structural Engineering and Construction

A Study on the Flexural Behavior of CFRP Box Beams with Different Laminate Structures

Hiroki Sakuraba^a, Takashi Matsumoto and Toshiro Hayashikawa

Graduate School of Engineering, Hokkaido University, Japan

Abstract

The objective of this study is to examine the strength and deformation characteristics of CFRP box beams with different laminates. Four CFRP box beams were fabricated with different laminate structures, and they were tested under four point bending. Their laminates consist of 25 laminae with different lamina proportion in longitudinal, transverse and diagonal direction. Displacements and strains were measured and those are compared to theoretically estimated results.

Strength is enhanced with a proper lamina proportion in longitudinal and diagonal direction. Three failure modes with different laminate structures are observed: (1) vertical cracking of web in specimens consisting of longitudinal and transverse laminae, (2) delamination of web in specimens including diagonal laminae, (3) combination between vertical cracking and delamination of web in a specimen composed of all lamina directions.

Shear deformation of the beams significantly contributes to their whole displacements. In order to increase flexural stiffness, using diagonal laminae are effective. Also, theoretically estimated displacements and strains based on classical lamination theory and Timoshenko's beam theory agree well with the experimental results.

Keywords: CFRP box beam; laminate structure; strength; failure mode; deformation

^a Corresponding author and presenter: Email: sakuraba_h@eng.hokudai.ac.jp

1. INTRODUCTION

Corrosion of steel beams in bridges due to severe salt environment is a significant problem to maintain the bridges. As repainting in the beams is required during their service period, Life Cycle Cost (LCC) is increased. Recently, saving of LCC is an important focus, and it needs to be further improved.

Carbon fiber reinforced polymer (CFRP) with non-corrosive nature and high strength is recognized as a more durable material than steel to solve the problem. Because of the advantage, CFRP laminate is expected as a beam that replaces steel beams under severe environment.

However, the CFRP laminate has an anisotropic nature because it is fabricated by stacking a number of laminas with various orientations in the thickness direction. The design of the fabrication is called “laminate structure”. Difference of how to stack and orient the laminas affects its material property. Therefore, a proper design method of the laminate structure for the beam is necessary, but it is not well established yet since CFRP is a relatively new material for civil engineering structures.

As one of the attempts to apply CFRP as a primary structural member in Japan, Mutsuyoshi et al. (2007) [1] carried out a bending test of I-shaped hybrid girders consisting of CFRP and GFRP (Glass Fiber Reinforced Polymer). Sugiura and Kitane (2009) [2] investigated a flexural behavior of CFRP box girders with trapezoidal cross section. They revealed the applicability of the hybrid girders and the CFRP girders, but those authors did not focus on their laminate structures sufficiently. In order to use CFRP as a primary structural member efficiently, the proper design method of laminate structure is significantly required.

The objective of this study is to examine the strength and deformation characteristics of CFRP box beams with different laminates. Four CFRP box beams are fabricated with different laminate structures, and they are tested under four point bending.

2. EXPERIMENTAL METHOD

2.1. Specimens and setup for bending test

Bending tests of four specimens were performed to investigate their flexural behaviors and failure modes. The specimens consist of laminates made of 25 laminas which are thin carbon fiber sheets impregnated with thermoset resin. Dimensions of the specimens and loading conditions are shown in Figure 1. All specimens have a square box cross section with 100mm height, 100mm width and 5mm thickness. Their span, shear span and flexural span are 850mm, 375mm and 100mm, respectively.

Displacements and strains were measured at nine points and eight points, respectively as shown in Figure 2. Black arrows show displacement gauges (No.1 to No.9), and white arrows show loading points. No.7 and No.8 were set up to measure the settling of supports. No.5, No.6 and No.9 are to investigate the deformation of cross sections. Rosette gauges (No.1_s to No.6_s, the subscript S means strain gauges) and uniaxial gauges (No.7_s and No.8_s) are also illustrated. No.1_s and No.2_s are located at mid-shear span with mid-height to examine shear strain. No.3_s to No.6_s are to confirm the characteristics of a loading plate effect and to capture a precursor behavior of failure.

2.2. Laminate structure

Laminates of four beams have 25 laminas and different lamina proportion in longitudinal (0 degrees), transverse (90 degrees) and diagonal (± 45 degrees) direction. The angles are defined as shown in Figure 3. The 1-2 axes represent laminate axes and x-y axes show lamina (material) axes. Table 1 exhibits the laminate structures. For example, $[0/90]_6/0/[0/90]_6$, the first left side number means the lamina orientation

of the first layer. The subscript six indicates that six $[0/90]$ groups are continuously stacked. All of the laminate structures are symmetric about the mid-plane.

Names of the specimens are based on the proportion of each lamina orientation. Specimen No.1, No2, No.3 and No.4 are L1T1, L1D2, L1D1 and L1T1D2, where L, T and D representing longitudinal, transverse and diagonal, respectively.

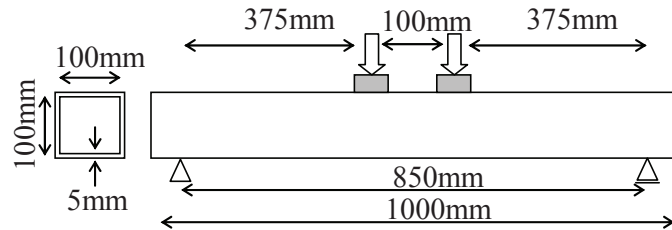


Figure 1: Dimensions of specimens and loading conditions

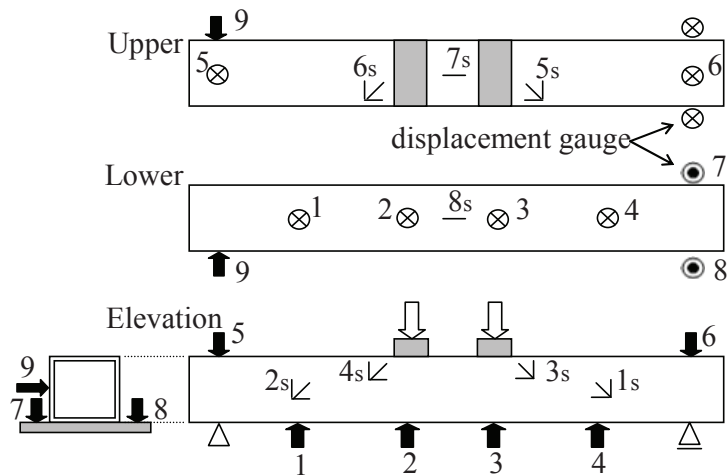


Figure 2: Setup for bending test

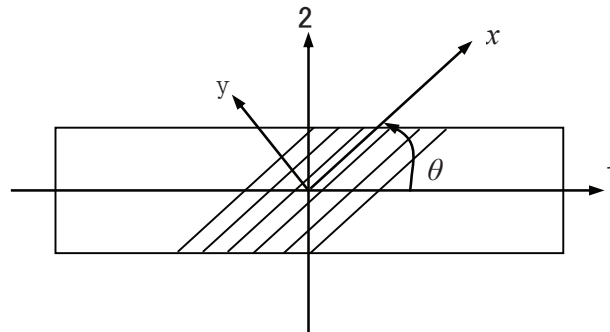


Figure 3: Laminate axes and lamina axes

Table 1: Laminate structure and specimen name

| No. | Laminate structure | Specimen name | The number of laminas | | |
|-----|--|---------------|-----------------------|------------------|-----------------|
| | | | Longitudinal (0°) | Transverse (90°) | Diagonal (±45°) |
| 1 | [0/90] ₆ /0/[0/90] ₆ | L1T1 | 13 | 12 | 0 |
| 2 | [0/45/-45] ₄ /0/[-45/45/0] ₄ | L1D2 | 9 | 0 | 16 |
| 3 | [0/45/-45/0] ₃ /0/[0/-45/45/0] ₃ | L1D1 | 13 | 0 | 12 |
| 4 | [0/45/-45/90] ₃ /0/[90/-45/45/0] ₃ | L1T1D2 | 7 | 6 | 12 |

3. EXPERIMENTAL RESULTS AND DISCUSSIONS

3.1. Strength and failure mode

Strength of L1T1, L1D2, L1D1 and L1T1D2 are 49.3kN, 64.6kN, 70.2kN and 62.5kN (Table 2), respectively. L1T1 without diagonal laminas shows the lowest strength and the other specimens with diagonal laminas have higher strength than L1T1. In the case of L1D1, although the number of diagonal laminas is the same as L1T1D2, L1D1 exhibits higher strength than L1T1D2. Also, by comparing L1D1 to L1D2, L1D1 with larger number of longitudinal laminas represents higher strength than L1D2. Therefore, it is concluded that a proper lamina proportion in longitudinal and diagonal direction is important in terms of enhancing their strengths in this experiment.

Failure modes are categorized as three types (Table 2), (1), (2) and (3) are observed: (1) vertical cracking of web in L1T1, (2) diagonal delamination of web in L1D2 and L1D1, (3) vertical cracking and delamination of web in L1T1D2. Their locations and pictures are shown in Figure 4 and Figure 5, respectively. The vertical cracking of web is caused in the case of having orthogonally oriented laminas in L1T1 and L1T1D2. Delamination of web takes place by using diagonal laminas in L1D2, L1D1 and L1T1D2.

3.2. Effective engineering properties

Effective engineering properties based on classical lamination theory are calculated to estimate theoretical displacements and strains which are based on Timoshenko's beam theory [3]. The estimated displacements and strains are compared to experimental results. Table 3 shows the lamina property and calculated effective engineering properties.

As a result, shear modulus G_{12} is increased in accordance with the increase of diagonal laminas and

Table 2: Strength and failure mode

| Specimen name | Strength (kN) | Failure mode |
|---------------|---------------|---|
| L1T1 | 49.3 | Vertical cracking of web |
| L1D2 | 64.6 | Diagonal delamination of web |
| L1D1 | 70.2 | Diagonal delamination of web |
| L1T1D2 | 62.5 | Vertical cracking and delamination of web |

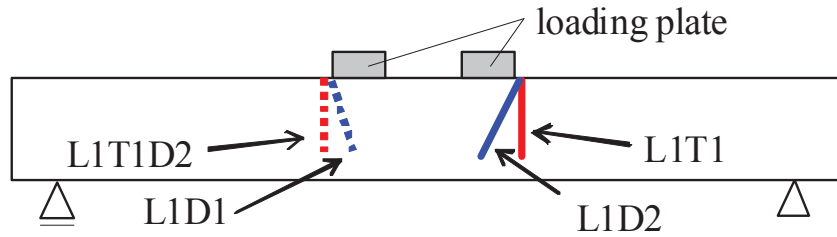


Figure4: Location of the failures (the opposite side of Figure 2)

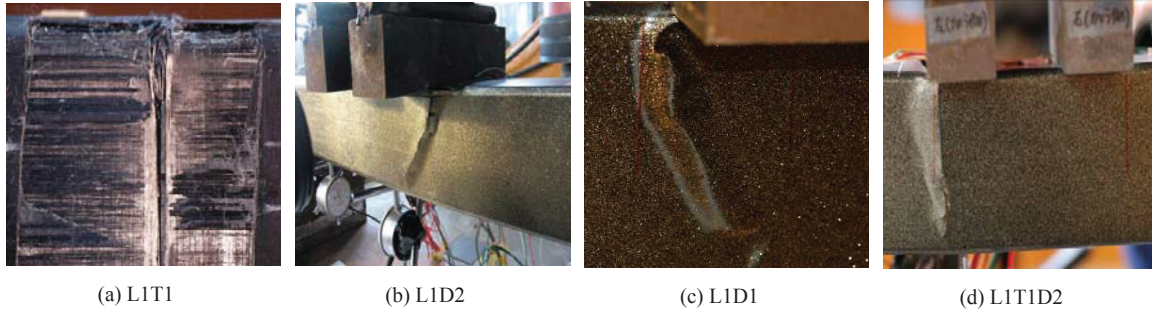


Figure 5: Failure mode

L1D2 shows the biggest G_{I2} . L1D1 and L1T1D2 have the same G_{I2} because of the same number of diagonal laminas. In the case of longitudinal modulus E_I , L1D1 and L1T1 exhibits around the same value, 74,420 MPa and 77,014 MPa, respectively. Actually, L1D1 shows bigger E_I because the contribution of diagonal laminas to longitudinal modulus is more effective than transverse laminas. Poisson's ratio ν_{I2} is lowered by using transverse laminas, L1T1 shows the lowest ν_{I2} . On the other hand, L1D2 and L1D1 show higher ν_{I2} , 0.677 and 0.630, respectively because of no transverse laminas.

Table 3: Material Properties

| Property | Direction | E (MPa) | G (MPa) | ν |
|----------------------------------|----------------|-----------|-----------|--------|
| Lamina | x | 128000 | 5600 | 0.32 |
| | y | 15200 | — | — |
| Effective engineering properties | Specimen names | | | |
| | L1T1 | L1D2 | L1D1 | L1T1D2 |
| E_I (MPa) | 74420 | 59450 | 77014 | 55233 |
| G_{I2} (MPa) | 5600 | 23634 | 19126 | 19126 |
| ν_{I2} | 0.070 | 0.677 | 0.630 | 0.326 |

3.3. Displacement

Flexural stiffness is increased by using diagonal laminas as shown in Figure 6 (those displacements are mean values between No. 2 and No.3), and L1D1 shows the smallest deflection. On the other hand, L1T1 exhibits the biggest deflection. At approximately 30kN level, displacement rates of L1D2, L1D1 and L1T1D2 to L1T1 are 76%, 62% and 86%, respectively. In every case, the relationship exhibits a linear

response up to 40kN. It seems that some damages took place after 40kN although they were progressive. Actually, in the experiment, longitudinal crackings near loading plate at corner between upper flange and web were observed visually in L1T1 at 38.9 kN and L1D2 at 40.1 kN. Upon the longitudinal crackings, a small sound like a fiber rupture was confirmed. Finally, the failures occurred as a brittle behavior.

Displacements calculated by equation (1) are also shown in Figure 6 (their legends are illustrated by specimen name plus t). As a result, the theoretical displacements agree relatively with the experimental results except L1T1. Contributions of shear displacement to whole displacement in L1T1, L1D2, L1D1 and L1T1D2 reach 39%, 11%, 16% and 12%, respectively. Therefore, in the case of L1T1, the shear displacement significantly affects its whole displacement due to smaller G_{12} resulting from no diagonal laminas.

$$w = w_b + w_s = \frac{P}{2E_1I} \left\{ \frac{a^3}{3} + \frac{a^2b}{2} \right\} + \frac{Pa}{2G_{12}kA} \quad (1)$$

where, w_b : flexural displacement, w_s : shear displacement, P : load, E_1 : longitudinal modulus, G_{12} : shear modulus, I : moment of inertia, A : cross section, k : coefficient of shear displacement ($=A/A_w=0.474$, A_w : cross section of web), a : shear span ($=375\text{mm}$), b : flexural span ($=100\text{mm}$).

Relationship between load and displacement of upper flange on the support is shown in Figure 7 (a) (those displacements are mean values between No. 5 and No.6) and Figure 7 (b) shows relationship between load and lateral displacement of mid-height on the support. As a result, the displacements in Figure 7 (a) (negative value represents settling) are almost constant up to 40kN. Afterwards, the slopes suddenly become smaller. In Figure 7 (b), the displacements at 5kN are in proportional to estimated Poisson's ratio ν_{12} (negative value represents contractive direction). After 40kN, the direction of displacement becomes dilative. Therefore, it is concluded that longitudinal cracking as mentioned above affects the deformation of cross section.

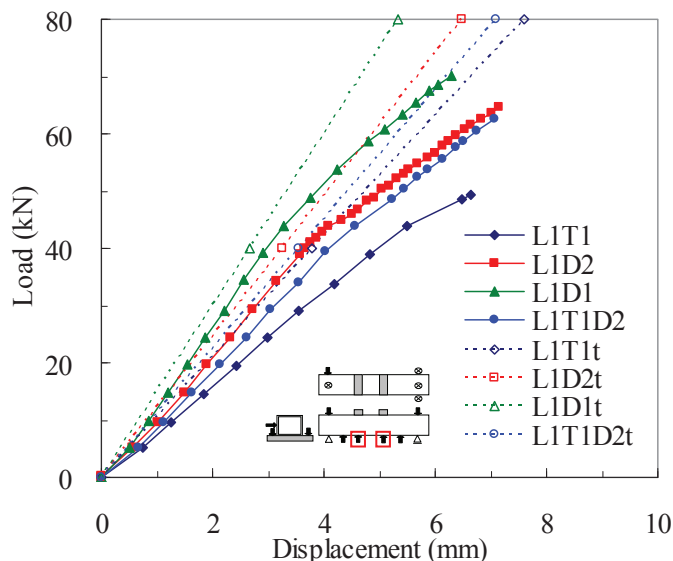


Figure 6: Load-displacement relationship at the loading point

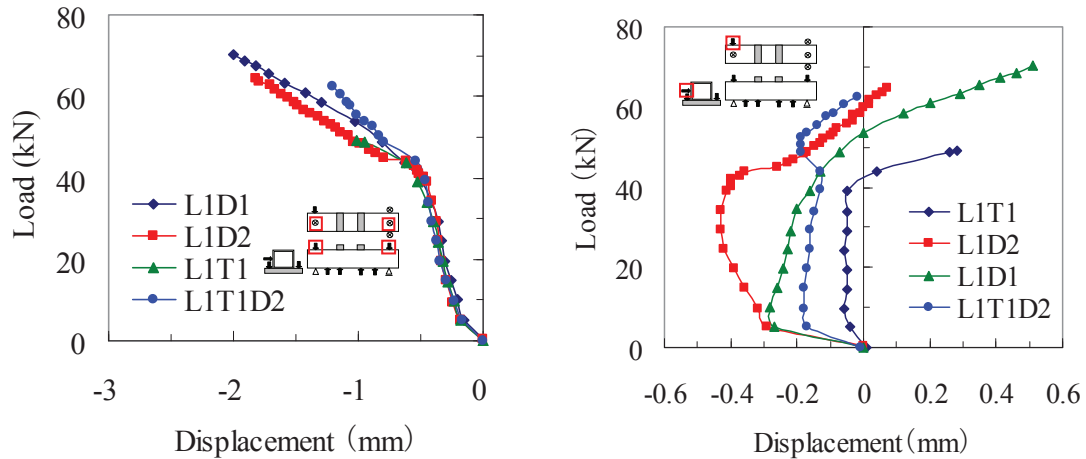


Figure 7: Load-displacement relationships on the support; (a) Vertical Displacement (No.5 and No.6) (b) Lateral displacement at mid-height (No.9)

3.4. Shear and longitudinal strain

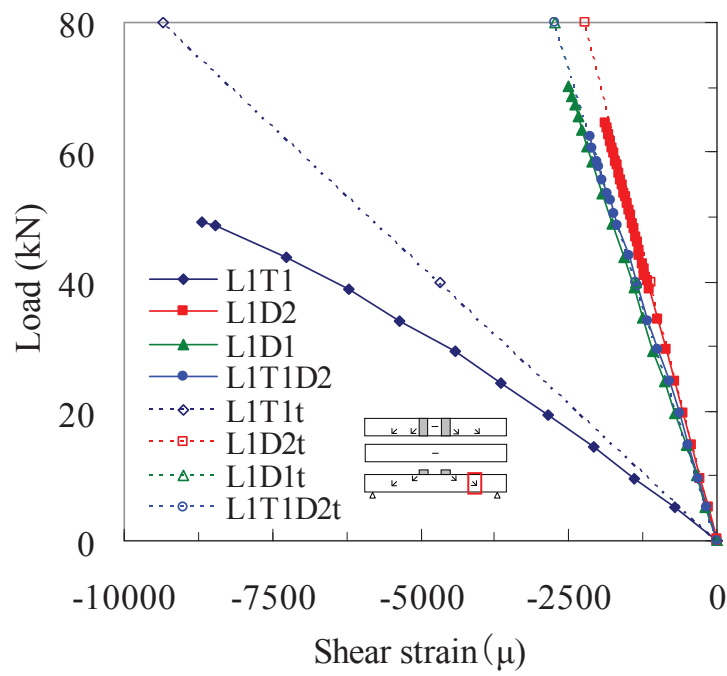
Shear strain and longitudinal strain are lowered by using diagonal and longitudinal laminas respectively, and it is also confirmed that the shear and longitudinal strain agree well with theoretically estimated results.

Relationship between load and shear strain at No. 1S and relationship between load and longitudinal strain at No.7S and No.8S are shown in Figure 8 (a) and (b), respectively. In Figure 8 (a), L1D2 exhibits the smallest shear strain due to the largest number of diagonal laminas. L1D1 represents the same slope as L1T1D2 because of the equal number of diagonal laminas. Also, theoretically estimated results correspond to the experimental results except L1T1. It seems that property of thermoset resin affects the response of L1T1 due to no diagonal laminas.

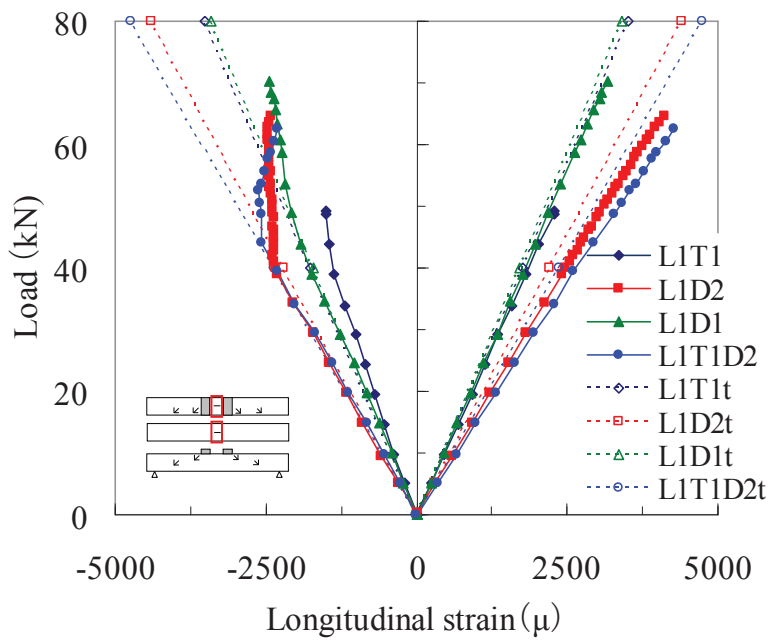
In Figure 8 (b), the curves at No.8S are linear response up to the failures. However, in the case of the curves at No.7S, the compressive strains after 40kN become almost constant. It seems that surface of the upper flanges do not transfer compressive stress furthermore due to some damages near the loading plates.

3.5. Principal strain

Figure 9 shows experimental and theoretically estimated principal strain in L1D2. According to the results, experimental principal strain on Upper at 19.7kN indicates the different direction to estimated one. It seems that the loading plates obstruct shear deformation of the flange. At 44.0kN after the longitudinal cracking as mentioned above, the strains do not show a linear behavior near the loading plates. Also, the principal strains at No.4S and No.6S near the left side loading plate where the failure occurred exhibit larger strain than No.3S and No.5S, respectively. Therefore, it is thought that the loading plates contribute to the longitudinal cracking and affect the deformation characteristics. Thus, a countermeasure is needed to prevent the longitudinal cracking in the future.



(a) Shear strain at No.1S



(b) Longitudinal strain at No.7S and No.8S

Figure 8: Load-strain relationships; (a) Shear strain at No.1S; (b) Longitudinal strain at No.7S and No.8S

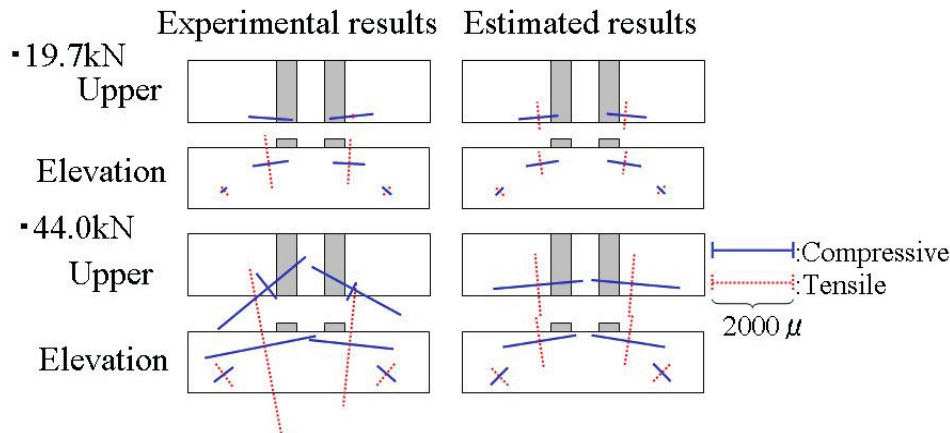


Figure 9: Principal strain in L1D2

4. CONCLUSIONS

Flexural behavior of CFRP box beams with four laminate structures were examined in this study. Four point bending tests were performed in order to investigate how their strength, failure mode and deformation characteristics are changed by using different laminate structures with the same dimensions and loading conditions. The conclusions are summarized as follows.

A proper lamina proportion in longitudinal and diagonal direction is important in terms of increasing strength. Specimen L1D1 exhibits the highest strength because of a suitable lamina proportion within this experiment.

Three failure modes are observed with different laminate structures and the failures occur near the loading plate. Vertical cracking of web is caused in the case of laminates consisting of orthogonally oriented laminas such as L1T1 and L1T1D2. Delamination of web takes place by using diagonal laminas in L1D2, L1D1 and L1T1D2.

Deformation of the beams is significantly affected by shear deformation. In order to increase flexural stiffness, using diagonal laminas are effective because shear modulus is enhanced, and indeed L1D1 shows the smallest deflection. Also, theoretically estimated displacements and strains by using Timoshenko's beam theory with effective engineering properties agree well with the experimental results.

ACKNOWLEDGMENTS

This research was supported partially by the Kajima Foundation's Research Grant. The authors acknowledge Toray Industries, Incorporated for the support in undertaking this study. The opinions expressed here are those of the authors and not necessarily those of Toray Industries, Incorporated.

REFERENCES

- [1] Hiroshi Mutsuyoshi, Thiru Aravinthan, Shingo Asamoto and Kenji Suzukawa (2007). Development of New Hybrid Composite Girders Consisting of Carbon and Glass Fibers, COBRAE conference 2007 Benefits of composites in civil engineering, 2, university of Stuttgart, Germany.

- [2] Kunitomo Sugiura and Yasuo Kitane (2009). Static Bending Test of Hybrid CFRP-Concrete Bridge Superstructure, Proceedings of US-Japan Workshop on Life Cycle Assessment of Sustainable Infrastructure Materials, Hokkaido University, Japan.
- [3] Hiroki Sakuraba, Takashi Matsumoto, Eigo Kido, Jyunichi Masago, Toshiro Hayashhikawa (2010). Study on the deformation behavior of CFRP box beams with lamina of 45 degrees under flexure, Proceedings of Hokkaido Chapter of the Japan Society of Civil Engineerings No.66, A-4, Japan.